Low temperature plasma channels generated in microcavity trenches with widths of 20–150 μm and aspect ratios as large as 10^4:1

M. Lu, S.-J. Park, B. T. Cunningham, and J. G. Eden[a)]
Department of Electrical and Computer Engineering, University of Illinois, Urbana, Illinois 61801, USA

(Received 18 October 2007; accepted 2 December 2007; published online 14 March 2008)

Low temperature plasma channels with widths as small as 20 μm, cross-sectional areas of 400–12 000 μm^2, and aspect ratios (channel length to width) of up to 10^4:1 have been generated on a steady state basis within sealed microcavity trenches fabricated by replica molding. With lengths up to 1 m and volumes of 10^{-5}–$\sim 10^{-2}$ cm^3, these channels are situated in a dielectric barrier structure having a transverse, buried electrode geometry and are sustained by power loadings as high as $\sim$1.2 kW cm^{-3}. Current densities of $\sim$5–10 A cm^{-2} and estimated electron densities of $\sim 10^{11}$–10^{13} cm^{-3} are produced with a 20 kHz sinusoidal voltage of V_{rms}=225–325 V, rendering these channels of interest as on-chip plasma reactors or nonlinear optical conversion media. With the transversely excited, photolithographically defined microcavity structures reported here, plasma channels of at least several meters in length, and having an arbitrary, folded geometric pattern, can be generated. © *2008 American Institute of Physics*. [DOI: 10.1063/1.2827197]

Plasma channels produced in atmospheric air or submillimeter diameter capillaries by pulsed optical fields at intensities typically $>10^{12}$–10^{13} W cm^{-2} are of fundamental and applied interest. Owing to competition between the optical Kerr effect and multiphoton ionization in channels generated by $\sim$100 fs Ti:Al_2O_3 laser pulses in air, filaments having diameters of nominally 10–150 μm are formed, which can extend over lengths of several meters.[1–3] Furthermore, pulsed microplasmas produced optically or electrically within capillaries (diameters of typically $<$200 μm) have become integral to rapid advancements in high order harmonic generation[4,5] (HHG) and extreme ultraviolet/soft x-ray lasers powered by optical field ionization[6] or a pulsed discharge.[7]

This letter reports the realization of low temperature plasma channels in high aspect ratio trenches of rectangular cross section fabricated by plastic-based replica molding. Generated on a continuous basis by a transverse geometry, dielectric barrier discharge structure, these channels have widths of 20–150 μm and volumes of 10^{-5}–$10^{-2}cm^3$. Channel lengths up to 1 m have been achieved to date, yielding aspect ratios of 10^4:1, and folding the channel into intricate geometric patterns has been demonstrated. The specific power loadings ($\leqslant$1.2 kW cm^{-3}) and narrow channel widths observed thus far suggest the utility of these microplasmas for on-chip chemical synthesis (such as the production of H_2 in Ar/NH_3 mixtures,[8] or O_3 generation), plasma remediation, and nonlinear optical spectroscopy.

Microcavity plasma devices[9] capable of confining a low temperature plasma within a rectangular trench were fabricated in polymer substrates by processes similar to those described recently by Lu *et al.*[10] Panel (a) of Fig. 1 is a cross-sectional diagram (not to scale) of a representative device structure. A 1 mm thick glass plate or a flexible polyester sheet (127 μm in thickness), coated with a 200 nm thick film of indium tin oxide (ITO), served as the substrate. Microplasma channel cavities were formed in a layer of ultraviolet-curable polymer with a daughter mold bearing a negative volume image of the desired microcavity pattern. Fabricated in polydimethylsiloxane by a Si master mold, the daughter is flexible which is desirable when removing the mold from a rigid substrate. The master mold was produced on a 100 mm (4″) diameter Si wafer by conventional photolithographic and dry etching processes. Microchannels with widths as small as 20 μm were fabricated, but all microchannel and gas feed channels were etched into the master mold to depths of 80 and 20 μm, respectively. Following the replication of the cavity pattern, the liquid polymer was cured at 300 K for 30–90 s with an ultraviolet-emitting Xe source. A thin ($\sim$500 nm) dielectric film of TiO_2, SiO_2, Ta_2O_5, or Si_3N_4 was subsequently evaporated onto all interior surfaces of the microchannels and adjoining gas flow channels. The dielectric film serves several functions, one of which is to provide a barrier against the diffusion of organic vapors from the plastic host into the plasma cavity. Figure 1(b) is a scanning electron micrograph (SEM) of a portion of an array of 15 μm thick ribs spaced by $\sim$23 μm, illustrating the smooth morphology of the walls (and floor) attainable with replica molding. The 40 μm wide channel intersecting the array is designed for evacuation and gas filling purposes.

The upper section shown in Fig. 1(a), comprising a second polyester sheet coated with ITO and a dielectric film is bonded to the polymer cavity so as to fully seal the channels. After bonding the two sections of the device, electrical leads were attached to the film electrodes and the channels were evacuated to $\sim 10^{-6}$ Torr and backfilled with research grade gas. Because of the low gas pumping speed associated with the small cross-sectional areas of these channels (400–12 000 μm^2), high purity Ne or Ar was flowed through the structure until spectra were free of contaminant emission. Unless noted otherwise, all data were obtained by driving the channels with a 20 kHz sinusoidal voltage waveform.

A decided asset of replica molding for fabricating microplasma devices is the access provided to the study of plasma channels, bounded by a dielectric and having virtually any microgeometric cross-sectional structure and length. Optical micrographs of two examples are presented in Figs. 2 and 3. Fabricated from a 100×80 μm^2 rectangular cross-section channel, the folded rectangular pattern of Fig. 2 has an overall channel length of 0.25 m and is operating in 500 Torr of

a)Electronic mail: jgeden@uiuc.edu.

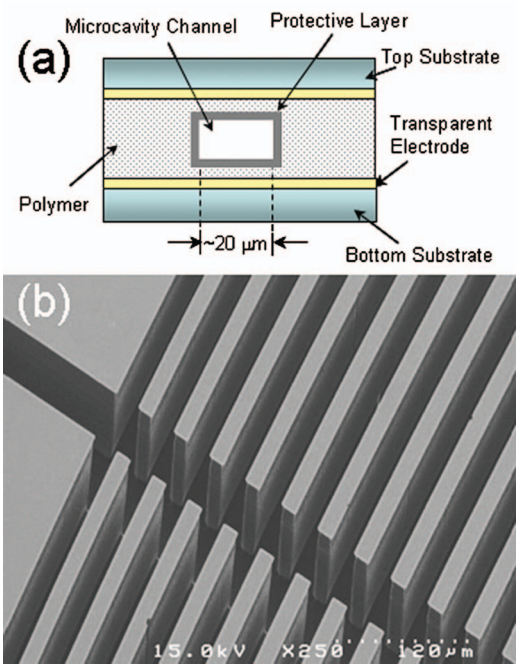

FIG. 1. (Color) (a) Diagram (not to scale) in cross section of a microchannel plasma structure fabricated by replica molding; (b) SEM of a portion of an array of 15 μm thick barriers (ribs) formed by replica molding. The width of the channels between the barriers is ~23 μm.

Ne. A circular spiral structure comprising a 150 μm wide channel with a depth of 80 μm and a length of 1 m is shown in Fig. 3. Operating in 500 Torr of Ar, this channel has an aspect ratio (length to width) of ~6700:1 and an active volume of 1.2×10^{-2} cm^3 (12 μL). To date, diffuse, uniform glows have been generated in channels with cross sections as small as 20×20 μm^2 and aspect ratios as large as 10^4:1. Emission over virtually all the channel of Fig. 3 is uniform

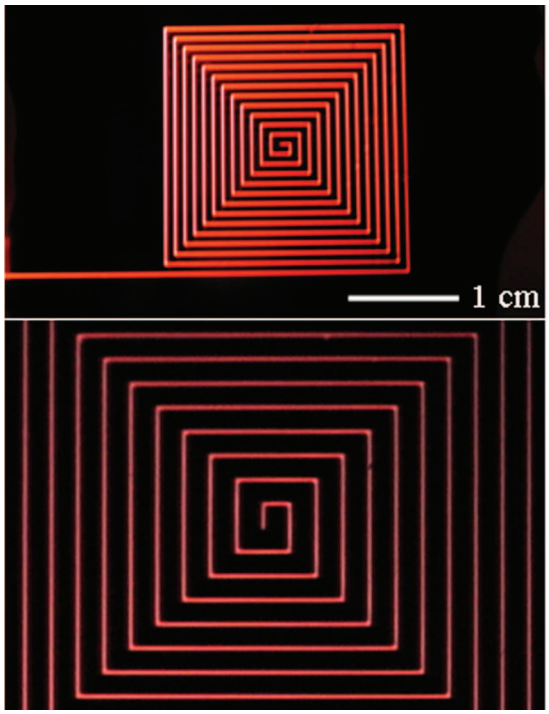

FIG. 2. (Color) Optical micrographs (at two values of magnification) of a square-folded microchannel with a 100×80 μm^2 cross section and an overall length of 0.25 m. The channel is shown operating in 500 Torr of Ne with a 20 kHz driving voltage of 325 V rms.

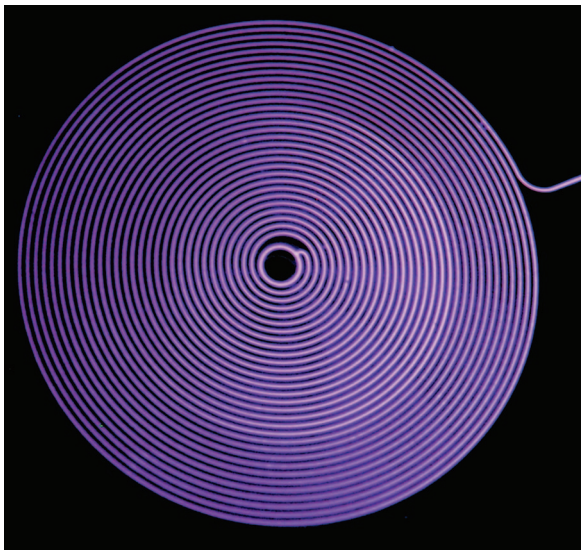

FIG. 3. (Color) Photograph of a spiral microplasma channel having a length of 1 m and transverse dimensions of 150×80 μm^2. The operating conditions are p_{Ar}=500 Torr and V_{rms}=310 V (20 kHz).

although a loss of a factor of 2 in intensity is evident at the perimeter of the spiral. Producing stable, spatially uniform plasmas in microchannels 1 m in length is unprecedented and is largely a result of orienting the electric field orthogonal to the plane of the folded channels of Figs. 2 and 3.

Voltage-current (V-I) characteristics for the spiral microchannel plasma of Fig. 3 are presented in Fig. 4 for Ne pressures between 500 and 800 Torr. Breakdown voltage for all of the pressures studied is ~225 V and it is evident that the conductivity of the microchannel varies little with pressure over the entire range investigated. After correcting for the displacement current, one can estimate the time-averaged electron density n_e from the conduction current shown by the inset to Fig. 4. For V_{rms}=250 V and $I_{rms}\sim1$ mA, the current density J and electric field strength E are ~8.3 A cm^{-2} and 31 kV cm^{-1}, respectively. Since the electron mobility μ_e is given by $q/m_e(\nu_m+j\omega)^{-1}$ (where q, m_e, ν_m, and ω are the charge on an electron, the electron mass, the collision fre-

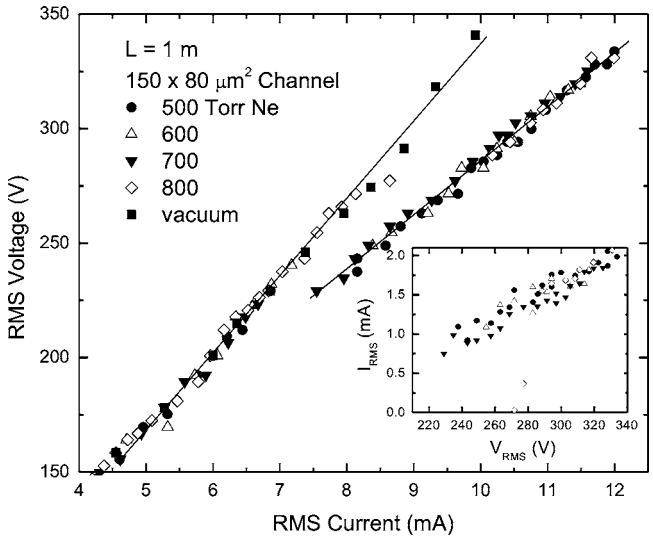

FIG. 4. Voltage-current (V-I) characteristics for the spiral channel of Fig. 3. Data are given for Ne pressures between 500 and 800 Torr, and the vacuum characteristic is also shown. For $p_{Ne}<700$ Torr, breakdown occurs at ~225 V rms. The inset displays the conduction current that is calculated by accounting for the displacement current.

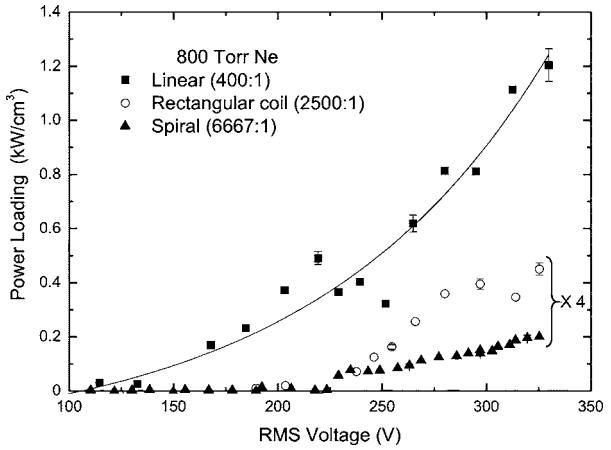

FIG. 5. Variation of the power loading with the rms driving voltage for a linear channel (2 cm in length), as well as the rectangular coil and spiral microchannels of Figs. 2 and 3, respectively. The devices were operated in 800 Torr of Ne and the values of power loading for the rectangular and spiral structures have been scaled by a factor of 4. The aspect ratio for each channel is given in parentheses in the upper portion of the figure.

quency for momentum transfer, and the plasma driving frequency, respectively) and $\nu_m \simeq 10^9\ \mathrm{s}^{-1} \cdot p_{\mathrm{Ne}}$ (expressed in Torr) $\geqslant \omega$, then μ_e is estimated from the $\omega \rightarrow 0$ (dc) expression to be $\sim 3 \times 10^3\ \mathrm{cm}^2\ \mathrm{V}^{-1}\ \mathrm{s}^{-1}$. Consequently, $n_e \sim 6 \times 10^{11}\ \mathrm{cm}^{-3}$. Although these values must be viewed as order of magnitude only, the estimated electron density is consistent with the principle that the steady state sustenance of a low temperature plasma in a channel demands that the transverse dimensions of the cavity be able to, at a minimum, accommodate twice the sheath thickness. This implies further that the Debye length λ_D be no larger than 15–20 μm which yields $n_e \sim (1.4\text{–}2.4) \times 10^{11}\ \mathrm{cm}^{-3}$ if the electron temperature T_e is 1 eV. Similar considerations suggest that n_e in the 20 μm square microchannels is not less than $\sim 10^{13}\ \mathrm{cm}^{-3}$. Indeed, it was found experimentally that, for a fixed Ne pressure, producing a uniform glow in the $20 \times 20\ \mu\mathrm{m}^2$ channels required an rms voltage ~57% higher than that necessary for a 150 μm wide, 1 m spiral channel.

Detailed measurements of the *V-I* characteristics for the three microchannel geometries reported here (rectangular coil of Fig. 2, spiral of Fig. 3, and linear channels with $20 \times 20\ \mu\mathrm{m}^2$ cross sections) reveal that power consumption does not scale linearly with volume. The 1 m long spiral channel, for example, consumes 0.5 W for $V_{\mathrm{rms}} \simeq 310$ V, whereas corresponding values for the rectangular coil and a linear channel, 2 cm in length, are 200 and 40 mW, respectively. Consequently, as illustrated in Fig. 5, power *loading* of the linear, $20 \times 20\ \mu\mathrm{m}^2$ cross-section channel is more than an order of magnitude larger than corresponding values for its more intricate design counterparts. Although the respective volumes for the three channels are in the ratio 1:25:150, the power dissipated in the linear channel is $\sim 1.2\ \mathrm{kW\ cm}^{-3}$ for $V_{\mathrm{rms}} \simeq 325$ V or a factor of ~12 greater than that for the rectangular coil. This result is attributable to several factors, one of which is: (1) the large electric field required to simply sustain a plasma in the $20 \times 20\ \mu\mathrm{m}^2$ channel.

Owing to the properties described above, microchannel plasmas are attractive for on-chip plasma reactors or the microanalysis of gas or vapor samples. Experiments with rare gas/(0.5–4)% CH_4 mixtures, for example, have been conducted with $200 \times 80\ \mu\mathrm{m}^2$ channels and, in accord with the results of Ref. 11 for Ar diluent, $A^2\Delta \rightarrow X^2\Pi$ emission from the CH radical [$(v',v'')=(0,0)$ peaks at ~431.4 nm] dominates the Swan bands of C_2 in Ne/CH_4 mixtures. Interestingly, optical emission spectroscopy also reveals a remarkable sensitivity of $Ne^* \rightarrow CH_4$ excitation transfer (* denotes an excited state) to the ion core of the Ne excited species. The well known $3p \rightarrow 3s$ emission lines of Ne, involving Rydberg states having the $^2P_{3/2}$ ion core, vanish with the addition of CH_4 concentrations >0.5% to a Ne microchannel plasma at a pressure of several hundred Torr. In contrast, the Ne $3p'[1/2]_0 \rightarrow 3s'[1/2]_1$ transition (585.25 nm in air), associated with the $^2P_{1/2}$ ion core, remains strong. With the addition of CH_4 to the gas flow stream, therefore, the plasma is bright yellow to the eye. The relative energies of the $3p$ and $3p'[1/2]_0$ states suggest that the Ne core configuration, and not the internal energy of the donor atom, is the primary determinant of the excitation transfer cross section.

In summary, microplasma channels having transverse dimensions as small as 400 $\mu\mathrm{m}^2$ have been fabricated in plastic-based substrates by replica molding and operated in the rare gases. Channel lengths and aspect ratios up to 1 m and 10^4:1, respectively, have been realized. Both the scientific and technological opportunities afforded by these microchannels appear to be considerable. With transverse dimensions approaching those for a single mode optical waveguide in the visible, microplasma channels will permit (albeit with an altered polymer/dielectric structure) waveguiding in pulsed microplasmas, which suggests intriguing opportunities for guiding intense laser beams for laser accelerator and HHG experiments. With regard to the latter, the internal dimensions of the channel can readily be modulated by replica molding, thereby optimizing the dramatic enhancements in the intensities of selected harmonics that are known[5,12] to result from phase matching in periodic structures. The capability of producing microplasma channels with lengths ⩾1 m is particularly promising for pursuing nonlinear spectroscopic processes characterized by low cross sections.

The technical assistance of J. Zheng, T. Anderson, and K. Collier, and the support of this work by the U.S. Air Force Office of Scientific Research are gratefully acknowledged.

[1] A. Braun, G. Korn, X. Liu, D. Du, J. Squier, and G. Mourou, Opt. Lett. **20**, 73 (1995).
[2] P. Sprangle, J. Peñano, B. Hafizi, and C. Kapetanakos, Phys. Rev. E **69**, 066415 (2004).
[3] J. Philip, C. D'Amico, G. Chériaux, A. Couairon, B. Prade, and A. Mysyrowics, Phys. Rev. Lett. **95**, 163901 (2005).
[4] See, for example, M. Nisoli, S. De Silvestri, O. Svelto, R. Szipöcs, K. Ferencz, Ch. Spielmann, S. Sartania, and F. Krausz, Opt. Lett. **22**, 522 (1997).
[5] A. Paul, R. A. Bartels, R. Tobey, H. Green, S. Weiman, I. P. Christov, M. M. Murnane, H. C. Kapteyn, and S. Backus, Nature (London) **421**, 51 (2003).
[6] B. E. Lemoff, G. Y. Yin, C. L. Gordon III, C. P. J. Barty, and S. E. Harris, Phys. Rev. Lett. **74**, 1574 (1995).
[7] J. J. Rocca, V. Shlyaptsev, F. G. Tomasel, O. D. Cortázar, D. Hartshorn, and J. L. A. Chilla, Phys. Rev. Lett. **73**, 2192 (1994).
[8] R. A. Arakoni, A. N. Bhoj, and M. J. Kushner, J. Phys. D **40**, 2476 (2007).
[9] K. H. Becker, K. H. Schoenbach, and J. G. Eden, J. Phys. D **39**, R55 (2006).
[10] M. Lu, S.-J. Park, B. T. Cunningham, and J. G. Eden, IEEE/ASME J. Microelectromechan. Sys. **16**, 1397 (2007).
[11] A. Yanguas-Gil, K. Focke, J. Benedikt, and A. von Keudell, J. Appl. Phys. **101**, 103307 (2007).
[12] E. A. Gibson, A. Paul, N. Wagner, R. Tobey, D. Gaudiosi, S. Backus, I. P. Christov, A. Aquila, E. M. Gullikson, D. T. Attwood, M. M. Murane, and H. C. Kapteyn, Science **302**, 95 (2003).